Available online at www.sciencedirect.com
ScienceDirect
Journal of Magnetic Resonance 187 (2007) 78–87
JMR Journal of Magnetic Resonance
www.elsevier.com/locate/jmr

^{1}H and ^{129}Xe NMR absorption line shapes in the presence of highly polarized and concentrated xenon solutions in high magnetic field

Denis J.-Y. Marion [a], Gaspard Huber [a], Lionel Dubois [b], Patrick Berthault [a], Hervé Desvaux [a,*]

[a] *Laboratoire de Structure et Dynamique par Résonance Magnétique, Service de Chimie Moléculaire, URA CEA/CNRS 331, CEA/Saclay, 91191 Gif-sur-Yvette, France*

[b] *Service de Chimie Inorganique et Biologique, CEA/Grenoble, 17 avenue des Martyrs, 38054 Grenoble, France*

Received 16 February 2007; revised 6 April 2007
Available online 13 April 2007

Abstract

The presence of highly concentrated dissolved laser-polarized xenon (~1 mol/L, polarization up to 0.2) induces numerous effects on proton and xenon NMR spectra. We show that the proton signal enhancements due to ^{129}Xe–^{1}H cross-relaxation (SPINOE) and overall shifts of the proton resonances due to the average dipolar shift created by the intense xenon magnetization are correlated. Protons behave as very useful sensors of the xenon magnetization. Indeed the xenon resonances exhibit many features such as superimposition of narrow lines on the main resonance due to clustering effects, or such as a polarization-dependent line broadening that is tentatively assigned to the effects of temperature fluctuations that decorrelate some distant dipolar field effects from local interactions, transforming xenon spins from "like" to "unlike" spins. These spectral features make difficult the determination of the average dipolar field by means of the xenon resonance but have interesting consequences on the heteronuclear polarization transfer experiment in Hartmann–Hahn conditions (SPIDER).

Keywords: Hyperpolarized xenon; Distant dipolar field; SPIDER; SPINOE; Lineshape

1. Introduction

The inherent low sensitivity of NMR drives the renewed interest into highly polarized spin systems [1–4] used as sources of polarization for other spins [5–7]. NMR studies of highly polarized solid-state samples have shown that the interplay between dipolar Hamiltonians and density matrix in the strong spin order regime leads to a noticeable modification of the width, resonance frequency and shape of the absorption lines [8–11]. Still considering a highly polarized system in liquid state, the averaging of short-range dipolar interactions due to Brownian motions results in the sole conservation of long-range terms in the dipolar Hamiltonian. They induce special effects such as multiple-echoes [12], intermolecular coherences [13], or spectral clustering in hyperpolarized liquid ^{3}He or ^{129}Xe [14–17]. These peculiar effects have led to many theoretical developments [18–20] and even predictions: (i) the spin dynamics in the presence of polarized and concentrated spin systems and small static field inhomogeneities has been shown to be source of a chaotic and dynamic distribution of the magnetization along the sample volume [21]; (ii) in the case of highly polarized systems ($P > 0.1$), Walls et al. have shown by numerical simulations that the situation may become even more complicated since the resonance linewidth becomes dependent on the polarization and on the magnetization flip angle [22].

On the other hand, we have recently proposed the SPIDER experiment [7], which allows a polarization transfer from dissolved hyperpolarized xenon to a solute proton

* Corresponding author. Fax: +33 1 69 08 98 06.
E-mail address: herve.desvaux@cea.fr (H. Desvaux).

1090-7807/$ - see front matter © 2007 Elsevier Inc. All rights reserved.
doi:10.1016/j.jmr.2007.04.003

using the heteronuclear long-range dipolar couplings. This is achieved through a Hartmann–Hahn recoupling scheme and requires a large polarization and a large concentration of dissolved xenon. The promises offered by this new method have driven us to experimentally investigate the effect of the xenon magnetization on the ^{129}Xe and ^{1}H NMR spectra in a high resolution NMR spectrometer (11.7 T) required to provide chemical resolution. The highly polarized and concentrated xenon batch generates, in a non-spherical sample, a sizable average dipolar field which superimposes to the static magnetic field [10,18,23]. This field is then responsible for a measurable shift of the spectrum of every spin in solution. By analyzing the variations of the ^{1}H and ^{129}Xe resonance frequencies and linewidths, we report here the connection between long range effects due to this average dipolar field created by xenon magnetization, and local effects resulting from cross-relaxation with hyperpolarized xenon. In particular the correlations between (i) the ^{129}Xe magnetization (ii) the ^{1}H signal enhancement due to ^{129}Xe–^{1}H cross-relaxation (SPINOE) [5,24] and (iii) the ^{1}H resonance frequency are evidenced. The frequency and the linewidth of xenon resonance also depend on the xenon magnetization but in a much more complicated way due to the weakness of long distance dipolar couplings relative to fluctuations of Zeeman resonance frequencies. Consequences for the SPIDER experiments are drawn.

2. Experimental methods

2.1. ^{129}Xe hyperpolarization and solution mixing apparatus

Ninety-six percent of enriched ^{129}Xe from Chemgas was polarized by the spin-exchange method [1] using a home-built apparatus described in Ref. [25] based on a Spectra-Physics titanium–sapphire pumped laser. The experiment was run in batch mode and the xenon was gathered under its solid form in a U-shaped tube fitting inside a solenoid immersed in a liquid-nitrogen dewar. Typically for the present experiments, three to four batches were accumulated. Once in the fringe field of the high field NMR magnet, the xenon was transferred by cryo-condensation into the previously degassed NMR tube (1.6 mm inner diameter and 3 mm outer diameter from Cortec) closed by a J. Young valve. It contained 90 μL of *trans*-2 pentenal and methanol in 99.6% deuterated cyclohexane (Eurisotop). The solute concentrations varied between 1 and 5 mmol L^{-1}, depending on the experiments. The small tube volume and the high xenon solubility in this solvent induced a sizeable final xenon pressure of ca. 5 bar and hence a concentration of about 1 mol L^{-1} [26]. After addition of xenon, the tube containing the frozen solution was rapidly heated, thermostated by immersion in a liquid bath at the desired temperature and vigorously shaken. The tube was then put back into the high field NMR magnet and the magnetic field homogeneity was optimized by temporally locking the magnet. Typically, the NMR experiments started 2 min after introduction of the NMR tube inside the magnet. All these steps always led to a reduction by a factor around two of the xenon polarization compared to what we achieved with xenon in the gaseous phase inside the final 3 mm NMR tube.

2.2. Description of the NMR experiment

All experiments were performed on a Bruker Avance500 spectrometer with a static field of 11.7 T using Xwinnmr or TOPSPIN softwares. Except when explicitly mentioned, classical inverse double ^{1}H/broadband or triple ^{1}H/^{15}N/broadband resonance probeheads with 3-axis gradients were used. All experiments using cyclohexane as solvent were performed at the measured temperature of the room (293 K) in order to avoid temperature gradients as much as possible.

In order to simultaneously monitor the behavior of the ^{1}H and ^{129}Xe magnetization, we simply resorted to the pulse sequence of Fig. 1 which consisted in an alternation of ^{1}H and ^{129}Xe hard pulses, each one followed by a long acquisition (>1 s) in order to precisely define the resonance frequencies. The series of ϑ-angle pulses on ^{129}Xe separated by delays τ allowed the artificial decrease of its magnetization $\mathcal{M}_k^{Xe}$. After k pulses, it became:

$$\mathcal{M}_k^{Xe} = \mathcal{M}_0^{Xe} \cos^k \vartheta \exp \frac{-k\tau}{T_1^{Xe}} = \mathcal{M}_0^{Xe} \cos^k \theta \qquad (1)$$

with T_1^{Xe} the xenon longitudinal self-relaxation time, and $\mathcal{M}_0^{Xe}$ the initial xenon magnetization. In Eq. (1), we took benefit from the constant delay τ to define an apparent magnetization loss per xenon pulse: $\cos\theta$.

The ^{2}H lock channel was disconnected during the whole experiment in order to avoid any interference between the control of the magnet and the spin dynamics during the recording of the chemical shift variations on the successive ^{1}H and ^{129}Xe spectra. The whole duration of the experiment was long due to the long ^{1}H self-relaxation times and the incompressible delay needed by the spectrometer to switch between proton and xenon acquisitions. As a consequence, the quality of the field homogeneity might change along the experiment duration. Safe monitoring of the variations of the ^{1}H and ^{129}Xe linewidths as a function of xenon magnetization was hence obtained by

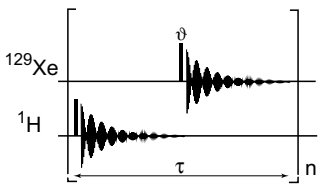

Fig. 1. Pulse sequence used to measure the average dipolar field created by laser-polarized xenon and experienced by protons. It consists in an alternation of ^{1}H and ^{129}Xe acquisitions. τ is the delay between two consecutive ^{1}H or ^{129}Xe pulses. The small-filled boxes correspond to hard pulses (90° flip-angle for ^{1}H and ~20° for ^{129}Xe).

adapting the pulse sequence of Fig. 1, for instance through acquiring multiple xenon spectra instead of one. This allowed a larger reduction of the xenon magnetization between two consecutive ^{1}H spectra, while avoiding non-linear response of the electronic circuit.

Since the delay τ was shorter than proton self-relaxation times T_1^H, for quantitative exploitation of proton signal intensity (SPINOE) we used ^{1}H 90° hard pulse in the sequence of Fig. 1. Moreover we acquired an extra (dummy) proton spectrum at the beginning of the experiment to destroy the initial proton magnetization and accelerate the establishment of a steady-state.

2.3. Data processing

All spectra were processed through Xwinnmr or TOPSPIN software from Bruker. The series of ^{1}H and ^{129}Xe spectra were first reorganized as two two-dimensional spectra. FIDs were zero-filled to 64k points, before Fourier transformation. The final digital resolution (Hz per point) was ca. 82 mHz for the ^{1}H spectra and 230 mHz for the ^{129}Xe spectra. The full width at middle height was less than 1 Hz for some proton resonances. If needed for improving the signal to noise ratio or for removing the effect of signal truncation (case of the ^{129}Xe spectra), a small exponential function (line broadening on the order of 0.3 Hz) was used for apodization. The same phase corrections were used for all ^{1}H and ^{129}Xe spectra along each series.

Post-processing of the spectra was performed using a home-written software. Peak frequencies were determined by fitting a parabolic function to all data points which intensities were higher than 80% of the point of highest intensity [27]. The fitting procedure was based on a Levenberg–Marquardt algorithm [28]. Through Monte-Carlo simulations, an estimation of the error on the peak frequency was derived. The peak signal intensities were determined by numerical integration of the signal. Since the resonance line could be non-Lorentzian, the resonance linewidths were simply determined by computing the number of points at various levels of intensity relative to the peak maximum.

The determination of the average dipolar field experienced by proton or xenon was obtained by fitting the function $f(k)$ to the experimental variations of peak resonance frequencies:

$$f(k) = A\cos^k\theta + B \tag{2}$$

where θ corresponded to the decrease of xenon magnetization due to hard pulses and relaxation (Eq. (1)). A was the average dipolar shift and B was the proton or xenon resonance frequency in the absence of polarized xenon. Similarly, for the SPINOE contributions to the signal (variations of proton signal intensities), the same function was used, but then A and B corresponded to the maximum enhancement due to SPINOE and the steady-state signal intensity, respectively. In the two cases, the uncertainties on A and B were determined by Monte-Carlo simulations using the errors computed at the previous step. In the case of SPINOE, since the proton T_1^H values are on the same order of magnitude as the interscan delay $\tau \simeq 21.7$ s, it might happen that a miscalibration of the ^{1}H 90° hard pulse delayed the establishment of the steady-state. By numerical simulations we observed that it was then safer to increase the uncertainties associated to the two first proton spectra. The simulations revealed that in these conditions, the induced bias on the determination of θ was smaller than 0.11°.

3. Heteronuclear coupling: ^{1}H frequency shift and SPINOE

3.1. General aspects

A proton spin of a solute is coupled via dipolar interactions to all xenon spins present in solution. Its short-range interactions with neighbors are averaged out by the Brownian motion because of their dependence on the angle between the static magnetic field B_0 and the internuclear vector [29]. At long distances however, the Brownian motion becomes inefficient and thus the long range interactions have to be considered [10,12,13,18–21]. Due to their dependence on $1/r_{jk}^3$ with r_{jk} the distance between the proton j and the xenon k, their effect would be negligible if it was not for the very high polarization and concentration of xenon in solution. Indeed this sum of interactions leads to a non-negligible average dipolar field superimposed to the static field. Its magnitude in Tesla is [23]:

$$B_{Xe} = 1000\frac{\mu_0}{3}\xi c_{Xe}\mathcal{N}P_{Xe}\gamma_{Xe}\hbar \tag{3}$$

where $\mathcal{N}$ is the Avogadro's number, γ_{Xe}, c_{Xe} and P_{Xe} stand for the ^{129}Xe gyromagnetic ratio, concentration in mol L^{-1} and polarization level, respectively, and ξ is a numerical factor-dependent on the sample's geometry ($-1/2 < \xi < 1$). This field induces a shift δ_H of the ^{1}H resonance frequency

$$\delta_H = -\gamma_H B_{Xe} \tag{4}$$

proportional to the xenon magnetization per unit volume. Indeed Eq. (3) is obtained by assuming that the magnetization per unit volume is uniform along the sample.

3.2. Experimental features

The ^{1}H spectra of Fig. 2, acquired using the pulse sequence of Fig. 1, illustrated the typical behavior of proton spectra when xenon magnetization decreased as a consequence of small ^{129}Xe hard pulses. A significant time dependence of the central frequency (variation of 4.17 ± 0.10 Hz) and of the signal intensity (in gray scale) of the aldehyde ^{1}H doublet of pentenal was observed. The fact that in the second experiment inversion of the xenon polarization during the optical pumping step led to inversion of the proton chemical shift variation by the same amount proved that a possible spectrometer frequency drift cannot be at the origin of this effect.

In agreement with Eq. (2), a downfield shift was observed for xenon polarized with a positive spin

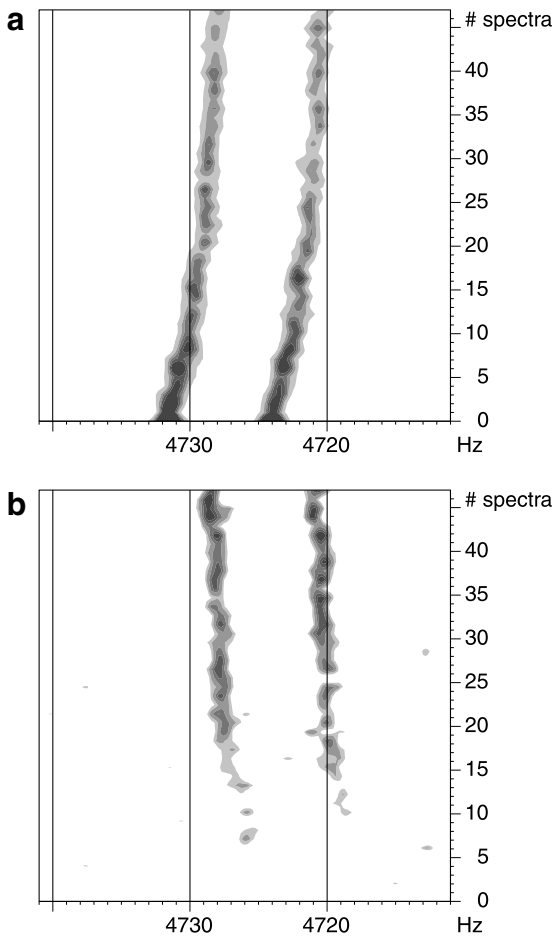

Fig. 2. Partial 2D contour plot of the variation of the ^{1}H frequency and intensity of the doublet of aldehyde proton of *trans*-2 pentenal dissolved in deuterated cyclohexane as a function of time. Between two consecutive ^{1}H spectra, a ~20° flip angle pulse was applied on ^{129}Xe (pulse sequence of Fig. 1). Xenon had either (a) positive or (b) negative spin temperature with a polarization of about 10%. SPINOE explained stronger (a) and lower (b) ^{1}H signals for the first spectra. The best-fit values of proton resonance frequency shifts due to the xenon magnetization were 4.17 ± 0.10 Hz and -4.23 ± 0.09 Hz, respectively.

temperature,[1] and the same shift was observed for all proton resonances. On the other hand, although for all protons the signals were subjected to either an increase of sensitivity for the first spectra in the case of xenon polarized with a positive spin temperature or a decrease of sensitivity when xenon spin temperature is negative, the variations of signal intensities were not the same. The presence of laser-polarized xenon affected the ^{1}H signal intensities because of SPINOE [5,24], which depends on the xenon–proton cross-relaxation rates σ_{XeH} but also on the proton self-relaxation times T_1^H. Indeed, using the simplest model, i.e. neglecting the mixing between xenon and proton magnetization build-up rates,[2] the proton magnetization $\mathcal{M}_k^H$ of the kth spectrum depended on the xenon magnetization $\mathcal{M}_k^{Xe}$ according to:

$$\mathcal{M}_k^H = \left(\mathcal{M}_0^H - \sigma_{XeH} T_1^H \mathcal{M}_k^{Xe}\right)\left(1 - e^{-\tau/T_1^H}\right) \quad (5)$$

The behavior of the proton signal intensities observed on Fig. 2 consequently arose from SPINOE.

Except for a possible unavoidable non-linear response due to radiation damping [30] after xenon excitation pulses in the case of negative spin temperature, the experimental results were qualitatively the same for positive and negative ^{129}Xe polarization. However, in order to avoid these non-linearities, we pushed further the data processing only for experiments with positive spin temperature.

3.3. Quantitative correlations

Even if the SPIDER experiments previously reported [7] had been acquired with xenon magnetization per unit volume on the order of that of Section 3.2, we have recently achieved higher xenon polarization in the gas phase (~50% instead of ~30%) thanks to the optimization of the laser beam, the purification of the xenon line, and a careful treatment (piranha solution, HF solution and coating by Surfasil) of a renewed glassware. These improvements have allowed us to increase the previously observed effects (Section 3.2). These larger effects allowed fine exploration of the interplay between the behaviors of xenon and proton magnetization. For all the rest of this text, all experimental data correspond to one of those experimental runs.

As illustrated in Fig. 3 the proton resonance frequency was linearly dependent on the xenon magnetization. At the beginning of the experiment, the proton resonance frequencies were shifted by about 9.5 Hz due to the average

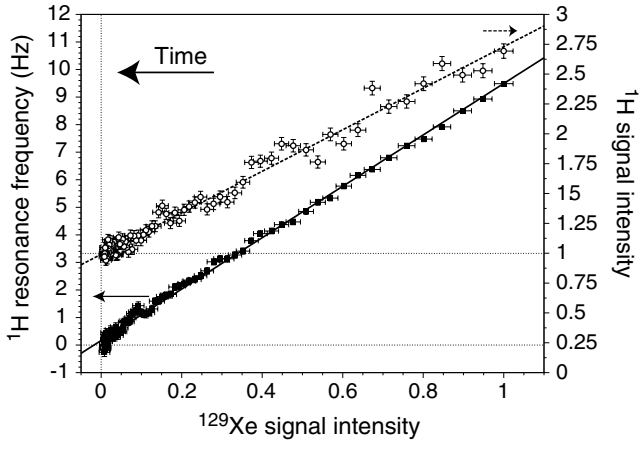

Fig. 3. Illustration of the linear correlations between the ^{1}H resonance frequency shifted due to xenon average dipolar field and the xenon signal intensity (closed squares) and between the ^{1}H signal intensity enhanced by xenon–proton cross-relaxation (SPINOE) and the ^{129}Xe magnetization (open circles). The plot corresponds to the aldehyde proton of *trans*-2 pentenal. Experimental conditions: ~1.3 mol/L of xenon polarized at 17% in deuterated cyclohexane at 293 K.

[1] γ_{Xe} is negative and $\xi = -1/2$ for an infinite cylinder.

[2] The assumption of decoupling resulted from the very long xenon T_1^{Xe} (measurements revealed values larger than 1500 s).

dipolar field created by xenon. Similarly, the proton signal intensity was a linear function of the xenon signal (Fig. 3). At the initial stage of the experiment, the proton signal was enhanced through SPINOE by a factor 2.7 relative to the steady-state signal using the same recovery delay τ and thermally polarized xenon. These large SPINOE enhancements and average dipolar field were obtained thanks to dissolved xenon with a polarization of 17% at the beginning of the ^{1}H and ^{129}Xe acquisitions.

More precise determinations of the average dipolar field or of the SPINOE experienced by any proton were performed by fitting the function $f(k)$ (Eq. (2)), with k the spectrum number, to the proton resonance frequencies and their signal intensities. Fig. 4 illustrated the quality of the agreement between the experimental results and this simple model which assumed that the xenon magnetization was reduced by a factor $\cos\theta$ between two consecutive proton spectra. Since the average dipolar field created by the ^{129}Xe magnetization was a long range effect, two different protons (aldehyde (a) and methyl (b) protons of pentenal) were experiencing the same upfield shift along the experiment as illustrated in Fig. 4a and b. From the best-fit theoretical curves to these two sets of points, the initial average field could be extracted. The values 9.39 ± 0.05 Hz for the case (a) and 9.37 ± 0.04 Hz for (b) were in perfect agreement. In fact, out of the 10 proton lines on which this fitting procedure could be performed due to sufficient intensity all along the experiment, 8 shift values ranged between 9.32 and 9.39 Hz. For the residual protonated solvent peak the fitted value was 9.09 ± 0.15 Hz but its associated uncertainty was large due to the short transverse-relaxation time of cyclohexane arising from chair–chair chemical exchange and unresolved coupling with deuterium. Finally, a value of 9.57 ± 0.04 was found for the OH peak of methanol. The discrepancy with the other average field values was likely to be due to a small temperature change during the whole experiment. This put an upper limit on the temperature drift during the experiment of about 0.05 K. For pentenal protons, no chemical shift variation with temperature could be detected.

As illustrated in Fig. 4c the amount of SPINOE contribution to the proton signal varied from one proton to another. For solute protons, the relative signal enhancement varied from about 0 for protons with short longitudinal self-relaxation times such as those of Surfasil to 2.0, i.e. observed signals 3 times greater than the steady-state ones. They were mainly correlated to the proton $T_1{}^{H}$ values (Eq. (5)). Taking as an example the aldehyde and methyl protons represented in Fig. 4, the best-fit signal enhancement factors due to SPINOE were 1.79 ± 0.03 and 0.80 ± 0.02 for T_1^{H} values of 33 ± 1 s and 18.3 ± 0.5 s, respectively. Based on Eq. (5), these two sets of values were in agreement, proving that a simple translational diffusion model for computing the dipolar correlation function [29] seemed to be well-adapted to treat the xenon–pentenal cross-relaxation. An even larger ^{1}H signal enhancement factor (11.1) was observed for C_6HD_{11} arising from its very long $T_1^{H} \simeq 120$ s. The ^{1}H signals corresponded to proton

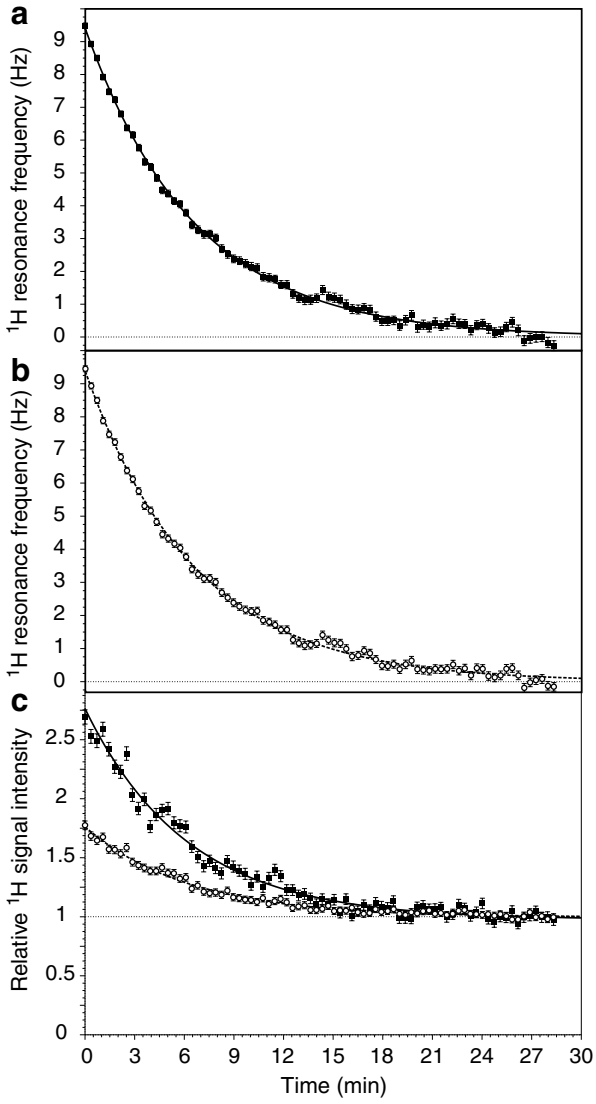

Fig. 4. Evolution of some proton resonance frequencies (a and b) and signal intensities (c) along the experiment of Fig. 3. Every 21.7 s a 19° pulse is applied on the xenon magnetization. The filled squares correspond to the aldehyde proton of *trans*-2 pentenal and the open circles to its methyl protons. The best-fit theoretical curves to Eq. (2) are superimposed. The time dependence of these two types of variation are almost identical. The proton resonance frequency shifts due to the average dipolar field created by xenon magnetization are identical (9.38 ± 0.05 Hz) while the signal enhancement factors due to SPINOE are different (1.79 ± 0.03 and 0.80 ± 0.02 for the aldehyde and methyl protons, respectively). The best-fit pulse flip angle values for the observed resonance frequency shifts are $18.66° \pm 0.25°$ and $18.67° \pm 0.21°$, and for the signal enhancement factors $19.29° \pm 0.31°$ and $19.06° \pm 0.47°$, respectively.

polarizations of 1.2×10^{-4} for protons of the solute and 5.0×10^{-4} for the solvent proton which, to the best of our knowledge, were the highest ever achieved through SPINOE [24].

3.4. Local and long range effects

The procedures used to fit the ^{1}H resonance frequencies and intensities to $f(k)$ gave access to the ^{129}Xe pulse flip

angle θ, which could be related to the average ^{129}Xe magnetization losses due to relaxation and hard pulse excitation between two consecutive proton spectra (Eq. (1)). On average the best-fit theoretical value for the proton resonance frequency was $\langle\theta_{\text{shift}}\rangle = 18.66° \pm 0.12°$ and for the effect on proton signal intensities[3] it was equal to $\langle\theta_{\text{SPINOE}}\rangle = 19.74° \pm 0.14°$. These two values differed by more than 1°. A pairwise comparison between all significant determined θ values (SPINOE larger than 40%) revealed that θ_{SPINOE} was systematically larger than the corresponding θ_{shift} (see caption of Fig. 4 for two examples). A Student's t-test validated the significance of the difference with a probability greater than 99.8% that it could not happen by chance. Similar behaviors were obtained in other experimental runs.

The interpretation of the discrepancy between these two θ values could be found in the nature of the interactions experienced by protons. On the first hand, the signal intensity of a proton was affected by the xenon spins present in its close neighborhood. On the other hand, the xenon dipolar field induced long range effects propagating over the whole sample. The sizeable difference between these two fitted values could consequently be explained by the effects of the pulses which decreased the xenon magnetization mainly inside the coils, letting parts of the sample located below or above the coils unaffected. The xenon pulses partially reduced the xenon magnetization inside the active volume of the xenon coil, while the whole xenon magnetization contributed to the average dipolar field experienced by protons. The global loss per pulse for the ^{129}Xe magnetization over the whole sample could then be smaller than the value inside the coil and the ^{1}H frequency shift then decreased less rapidly than the SPINOE enhancement. In fact, the respective values of θ_{SPINOE} and θ_{shift} could be expected to largely depend on the geometry of the sample and of the probe head.

4. Homonuclear coupling: ^{129}Xe resonance shift and linewidth

4.1. General features

Spectra of highly polarized xenon notably differ from those obtained with thermally polarized magnetization due to the effects of distant dipolar fields. As illustrated in Fig. 5 the typical profile of the xenon absorption line at a high polarization and concentration level exhibited a significant broadening (FWMH of approximately 8.1 Hz, compared to less than 1 Hz for ^{1}H resonances) and a sharp over-structure composed by a series of very well resolved peaks. Indeed, even if most of the transverse magnetization decayed in a short time, signal oscillations were definitely present after three seconds of acquisition. As already

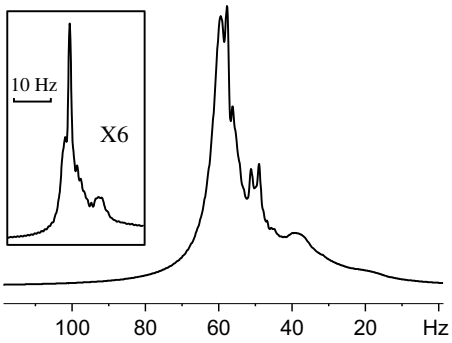

Fig. 5. ^{129}Xe NMR spectrum at the beginning of the experiment described in Fig. 3. Due to clustering effects, sharp resonance lines superimpose to the line which does not exhibit a Lorentzian shape. An arbitrary chemical shift reference is used. In insert, the 48th ^{129}Xe spectrum of the same experiment. The use of the same horizontal scale reveals the line narrowing.

reported [7,14–17], it was impossible to properly define T_2 for hyperpolarized species in liquids. So, the unusually broad ^{129}Xe line could not be the simple consequence of very short T_2, but rather the illustration of the existence of a frequency distribution in the sample. These features were characteristic of spectral clustering effects taking place at large magnetization levels [15,17,21]. Finally, as observed here, but also reported in the recent paper presenting the SPIDER experiment [7], the line broadening and the supplementary lines disappeared with the decrease of ^{129}Xe magnetization throughout the experiment.

4.2. Average dipolar field in the case of "like" spins

The average dipolar field created by N "like" spins S_i and experienced by the S spins is larger by a factor 3/2 than the effect experienced by any "unlike" spin [10]. Indeed, the dipolar Hamiltonian between two xenon spins S^i and S^j truncated by the effect of the strong Zeeman Hamiltonian in liquid phase is:

$$\mathscr{H}^{ij}_{\text{DD}} = d_{ij}(t)\left(S^i_z S^j_z - \tfrac{1}{4}(S^i_+ S^j_- + S^i_- S^j_+)\right) \tag{6}$$

If the two spins are "unlike", i.e. the difference of their resonance frequencies in the static magnetic field is larger than the dipolar coupling:

$$|\omega_j - \omega_i| \gg \mu_0 \hbar \gamma^2_{\text{Xe}}/4\pi r^3_{ij}, \tag{7}$$

based on perturbation theory, the flip-flop terms can safely be disregarded and dipolar Hamiltonian is reduced to the unique term:

$$\mathscr{H}^{ij}_{\text{DD}} = d_{ij}(t) S^i_z S^j_z \tag{8}$$

In the rotating frame, the time evolution of the xenon transverse magnetization proportional to $\langle S_+\rangle = \sum\langle S^i_+\rangle$, under the influence of the full dipolar Hamiltonian is given by:

[3] The large enhancement factor observed for cyclohexane induced that the associated best-fit θ_{SPINOE} value is significantly the best defined one. It consequently mainly defines the average value and associated uncertainty.

$$\frac{\mathrm{d}\langle S_+\rangle}{\mathrm{d}t} = 2\imath \sum_{j\neq k} d_{jk}(t)\left(\langle S_z^j S_+^k\rangle + \tfrac{1}{2}\langle S_+^j S_z^k\rangle\right) \tag{9}$$

In the right hand part of Eq. (9), the first term results from the $S_z^j S_z^k$ term and the second from the flip-flop terms.

We now apply the assumptions of distant dipolar fields in liquid state NMR [18–20,31,32] which allow one to write: $\langle S_\alpha^i S_\beta^j\rangle = \langle S_\alpha^i\rangle\langle S_\beta^j\rangle$ if S_i and S_j are two distant spins. Considering a given indiscernable spin $\langle S_+^j\rangle = \langle S_+\rangle/N$, Eq. (9) can thus be written as:

$$\frac{\mathrm{d}}{\mathrm{d}t}\langle S_+^j\rangle = 2\imath\left(\frac{3}{2}\sum_{k\neq j} d_{jk}\langle S_z^k\rangle\right)\langle S_+^j\rangle \tag{10}$$

$$= 2\imath \mathscr{M}_1^j \langle S_+^j\rangle \tag{11}$$

where the homonuclear first moment $\mathscr{M}_1^j$ is introduced. In Eq. (10), the flip-flop terms contribute through a factor 1/2 to the 3/2 coefficient. For any ellipsoidal distribution of spins S (or anything topologically equivalent) over which the concentration of "like" spins of type S is homogeneous, the first moment of the dipolar interactions is shown to be independent of the spin S_j taken as the origin [9,10,33]: $\mathscr{M}_1^j = \mathscr{M}_1^S$. It only depends on the geometrical factor ξ present in Eq. (3), and on the xenon concentration c_{Xe} and polarization P_{Xe}:

$$\mathscr{M}_1^S = 2\pi 1000\frac{\mu_0}{2}\xi c_{\mathrm{Xe}}\mathscr{N} P_{\mathrm{Xe}}\gamma_S^2\hbar \tag{12}$$

The analogy to Eqs. (3) and (4) is obvious with an enhancement by a 3/2 factor due to the flip-flop terms.

4.3. Xenon resonance frequency shift

We have explored the dependence of the ^{129}Xe resonance frequency on its polarization. For allowing comparisons, the series of ^{129}Xe spectra acquired in alternation to the proton ones discussed in Section 3.3 were considered. As fairly noticeable on Fig. 5, since for high polarization levels the xenon resonance line was not of Lorentzian shape, the definition of its resonance frequency was difficult. We consequently applied a small exponential function for apodization and considered the central resonance frequency of ^{129}Xe as the frequency obtained by fitting the highest peak to a parabolic function. As for the heteronuclear case, these central frequencies were found to be dependent on the xenon magnetization. Fig. 6 illustrated well the linear relation between these two values. Conversely to the proton case, the agreement was not perfect and in particular for this experiment a noticeable bump was observed during ca. 5 min on a whole experiment duration of about 28 min. The analysis of other experiments did not reveal the presence of this bump. We consequently concluded that it might result, on that particular experimental run, from external fluctuations like a slow and small variation of temperature (0.35 ppm/K i.e. 48.5 Hz/K) or of xenon concentration (slow setting up of the chemical equilibrium or liquid drop resulting from the initial shaking of the sample; xenon chemical shift variation [34]: 3.04 ppm mol^{-1} L). Apart from this bump, a very good correlation between ^{129}Xe polarization level and frequency shift was found. The best-fit value for the maximum frequency shift was equal to -5.37 ± 0.12 Hz. The bump as well as the problem of frequency determination in a non-Lorentzian resonance line limited the precision. In contrast, we expected a value of -3.9 Hz based on proton measurements, the difference of gyromagnetic ratios and the difference between "like" and "unlike" spins. The discrepancy was significant and confirmed in other experiments with values either too small or too large. Its origin remained unclear. Clues were the hypersensitivity of xenon chemical shift to temperature (assuming that the present difference only resulted from temperature, the extracted temperature drift would have been 0.03 K, a value in good agreement with that derived from the discrepancy between ^{1}H shifts and the methanol ones) or the problem of resonance line shape which would inhibit the correct definition of the central resonance frequency by simple fit of the peak of maximum intensity.

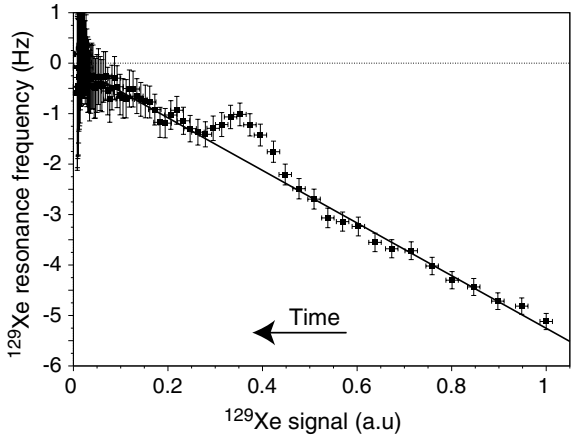

Fig. 6. Evolution of the ^{129}Xe frequency shift as a function of its magnetization revealing a linear correlation between these two values. The best-fit shift of the xenon line due to the average dipolar field it creates is -5.37 ± 0.12 Hz. Same experiment as this of Fig. 3.

4.4. Insights into the variation of the xenon linewidth

As recently mentioned [7], the behavior of the resonance linewidth of hyperpolarized species in liquids has been shown to be fully opposite to that observed for highly polarized system in solids. Whereas the resonance line was narrowed with increasing polarization in solid-state NMR [8,10], the opposite phenomenon was observed in liquids, hence the broad line visible Fig. 5. The monitoring of the xenon resonance as a function of polarization allowed us to better characterize this broadening. As illustrated in Fig. 7 for the experimental case of Fig. 3, for a large range of xenon magnetization, the xenon resonance line-width decreased with the polarization. Finally for the smallest polarizations the line seemed to broaden. Since

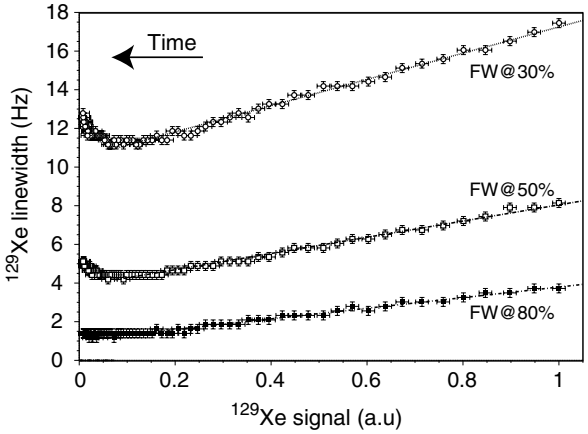

Fig. 7. Evolution of the ^{129}Xe NMR resonance linewidth as a function of the xenon magnetization. Since the resonance line shape is not Lorentzian, the xenon resonance linewidth is characterized by the full width (FW) at 80% of the maximum peak intensity (filled squares), 50% (open squares) and 30% (open circles). For large xenon polarization, linear relations between the xenon resonance linewidth and the magnetization are observed. Same experiment as Fig. 3.

the whole experiment has been acquired without any lock and any shim and as its duration was non-negligible (about 28 min), we have carefully checked the validity of these observations.

First of all, the study of other sets of experiments acquired on the same time scale or on a much more reduced one, always revealed the decrease of the linewidth with pulses for the high xenon polarizations, but the increase at low polarization could not be confirmed. The latter might result from the non-negligible uncertainty associated to the low signal to noise ratio of these spectra due to reduced xenon magnetization. Moreover, the same study on the variation of linewidths performed on the proton resonances did not reveal any significant line broadening whatever the xenon polarization. This proved that a whole degradation of the magnetic field homogeneity could not explain the observed effects. We have also checked that these behaviors for proton and xenon did not result from the particular geometry of the used probe (two different coils with xenon as the outer one). We have consequently performed this type of experiments on a ^{129}Xe/^{1}H double-tuned probe head. Similar significant line broadenings were observed for xenon magnetization at high polarization, which decreased with the polarization. At low polarization, line broadening for ^{1}H and ^{129}Xe resonances could not really be said to be significant whatever the experiment duration. This result suggests that the xenon line broadening at high polarization does not result from experimental artifacts.

We have experimentally checked that this line-broadening at high polarization neither resulted from a radiation damping effect [35,36] nor from distant dipolar field effects appearing with large pulse angles [22]. Indeed, at a given ^{129}Xe polarization, both the resonance line shapes and line-widths were identical whatever the ^{129}Xe flip angle in the range 1.5–20°. This result also showed a different behavior to that reported by Nacher et al. [15–17] since they observed a flip angle dependence. They tentatively assigned it to dynamical instabilities, as numerically predicted by Jeener but for larger flip angles [21]. The observed line-broadening hence results from a distribution of xenon resonance frequencies inside the sample which was correlated to the xenon polarization. The observed effect was opposite to that reported for solid-state samples. Moreover, the dependence on the polarization differed since in solids they were proportional to $\mathscr{M}_2^0(1-P_{Xe}^2)$, with $\mathscr{M}_2^0$ the second moment in the limit $P_{Xe}\to 0$ [8]. The present effect could consequently not result from dipolar broadening of the resonance line. On the other hand, its proportionality to the polarization made thinking that the observed effects were more related to the first moment $\mathscr{M}_1$ which is linearly dependent on the polarization P_{Xe} (Eq. (12)).

A model is consequently needed to explain this discrepancy on ^{129}Xe data, while a nice agreement between predictions and data is obtained for protons. The key difference between the derivations of the first moment in the homonuclear and heteronuclear cases comes from the flip-flop terms which have to be considered only in the first case (section 4.2). It remains that long range dipolar interactions induce small dipolar couplings, and difference of resonance frequencies might be non-negligible due, for instance, to differences of temperature. As an example considering two xenon spins separated by 1 mm and simply using the strong coupling condition (Eq. (7)) without considering any line-broadening contribution, in order for the flip-flop terms to be considered their difference of temperature should be typically smaller than 210^{-19} K. Due to this small value, they might not be correlated. Thus the resonance frequency of a given xenon spin would be defined by the sum of the average dipolar field created by distant spins considered as "unlike" spins due to temperature decorrelation and of the local field generated by the nearby xenon experiencing the same temperature, and which were consequently of "like" nature. Since these two fields were different (Eqs. (4) and (12)) and were dependent on the xenon polarization and on the geometry (geometric factor ξ in Eq. (12)), a distribution of ξ factors along the sample might be expected, resulting in the observed broadening of the xenon line at high polarization. The decrease of the polarization induces a decrease of the different first moments $\mathscr{M}_1$ and thus a narrowing of the line. Obviously in the case of protons, all xenon spins should be considered as "unlike", resulting in the existence of only one expression for the first moment $\mathscr{M}_1$ and one geometric factor ξ. This model consequently predicts, as observed, no broadening of the proton lines.

5. Conclusions

The presence of highly polarized and concentrated xenon in a solution affects many easily accessible NMR

parameters. We have shown that the ^{1}H signal enhancement due to SPINOE and the variation of ^{1}H resonance frequency are linearly proportional to the ^{129}Xe magnetization per unit volume. Their studies allow the determination of key parameters for SPIDER experiments such as the Zeeman resonance frequencies needed for applying on-resonance rf irradiations or the value of average dipolar field created by xenon spins. The characterization of xenon magnetization is, in fact, much easier by using proton as a sensor, which is less sensitive to non-linearities. Their origins are numerous for xenon. Some are well-documented as the non-linear coupling between high magnetization and the detecting coil (radiation damping) but others are much more tricky as the clustering effect which complicates the definition of the central line resonance frequency or induces the appearance of narrow lines superimposing the main resonance. Local field effects also affect the xenon resonance line shape through broadening. In particular, we show that it is proportional to the xenon polarization that we tentatively interpret as resulting from decorrelation between different parts of the sample due to tiny temperature fluctuations. The dipolar coupling between two distant xenon spins can indeed be either of "like" or "unlike" nature.

Interestingly, the detection of inhomogeneous xenon local fields by proton NMR is hardly possible in the reported experiments. Indeed the distribution of xenon rf fields along the sample might, at the end, create an inhomogeneous distribution of xenon magnetization per unit volume. It can consequently induce a distribution of local fields with physical properties different from a pseudo nuclear susceptibility shift, resulting in a distribution of ^{1}H resonance frequencies and thus in a broadening of ^{1}H resonance. No significant line broadening is detected. The xenon magnetization inhomogeneities may consequently be washed out along the experiment duration by spin or molecular diffusion. The only effect of xenon local fields on protons is finally indirectly detected through the difference of loss per pulses ($\cos\theta$ factor) measured by SPINOE and frequency shifts. Our results show that as experienced by protons in the present protocol, the dipolar field created by polarized xenon with positive spin temperature behaves almost perfectly as a pseudo nuclear susceptibility term for the simplest acquisition scheme.

For the SPIDER experiment, the present results predict difficulties to effectively benefit from all the xenon spin reservoir since parts of the sample may be decorrelated by temperature inhomogeneities. If a better understanding of the origin of the xenon line broadening might help, clues to circumvent these difficulties in SPIDER already exist, such as resorting to other hyperpolarized spin species with a smaller chemical shift dependency on temperature as ^{3}He or using multipulse recoupling schemes to compensate for the distribution of resonance frequencies [37].

Acknowledgments

We warmly thank Pr. Jean Jeener and Pr. Maurice Goldman for helpful comments. Bruker is greatly acknowledged for providing us the double-tuned $^{1}H/^{129}Xe$ probehead. We thank the Conseil Génral de l'Essonne for financial support (ASTRE program).

References

[1] T.G. Walker, W. Happer, Spin-exchange optical pumping of noble-gas nuclei, Rev. Mod. Phys. 69 (1997) 629–642.
[2] D.A. Hall, D.C. Maus, G.J. Gerfen, S.J. Inati, L.R. Becerra, F.W. Dahlquist, R.G. Griffin, Polarization-enhanced NMR spectroscopy of biomolecules in frozen solution, Science 276 (1997) 930–932.
[3] J.H. Ardenkjær-Larsen, B. Fridlund, A. Gram, G. Hansson, L. Hansson, M.H. Lerche, R. Servin, M. Thaning, K. Golman, Increase in signal-to-noise ratio of >10000 times in liquid-state NMR, Proc. Natl. Acad. Sci. USA 100 (2003) 10158–10163.
[4] J. Wolber, F. Ellner, B. Fridlund, A. Gram, H. Jóhannesson, G. Hansson, L.H. Hansson, M.H. Lerche, S. Møansson, R. Servin, M. Thaning, K. Golman, J.H. Ardenkjær-Larsen, Generating highly polarized nuclear spin in solution using dynamic nuclear polarization, Nucl. Instrum. Method A 526 (2004) 173–181.
[5] G. Navon, Y.-Q. Song, T. Rõõm, S. Appelt, R.E. Taylor, A. Pines, Enhancement of solution NMR and MRI with laser-polarized xenon, Science 271 (1996) 1848–1851.
[6] C.-G. Joo, K.-N. Hu, J.A. Bryant, R.G. Griffin, In situ temperature jump high-frequency dynamics nuclear polarization experiments: enhanced sensitivity in liquid-state NMR spectroscopy, J. Am. Chem. Soc. 128 (2006) 9428–9432.
[7] H. Desvaux, D.J. Marion, G. Huber, L. Dubois, P. Berthault, Direct enhancement of any solution NMR signal using the distant dipolar fields created by highly polarized and concentrated nuclear spin systems, Eur. Phys. J. Appl. Phys. 36 (2006) 25–34.
[8] A. Abragam, M. Chapellier, J.F. Jacquinot, M. Goldman, Absorption lineshape of highly polarized nuclear spin systems, J. Magn. Reson. 10 (1973) 322–346.
[9] Y. Roinel, V. Bouffard, First moments of NMR lines for highly polarized nuclei: a rigorous version of the "local field", J. Magn. Reson. 18 (1975) 304–319.
[10] A. Abragam, M. Goldman, Nuclear Magnetism: Order and Disorder, Clarendon Press, Oxford, 1982.
[11] J.S. Waugh, O. Gonen, P. Kuhns, Fourier transform NMR at low temperatures, J. Chem. Phys. 86 (1987) 3816–3818.
[12] G. Deville, M. Bernier, J.M. Delrieux, NMR multiple echoes observed in solid ^{3}He, Phys. Rev. B 19 (1979) 5666–5688.
[13] W.S. Warren, W. Richter, A.H. Andreotti, B.T. Farmer II, Generation of impossible cross-peaks between bulk water and biomolecules in solutions NMR, Science 262 (1993) 2005–2009.
[14] D. Candela, M.E. Hayden, P.J. Nacher, Steady-state production of high nuclear polarization in ^{3}He–^{4}He mixtures, Phys. Rev. Lett. 73 (1994) 2587–2590.
[15] B. Villard, P.J. Nacher, NMR spectral clustering and instabilities in polarised liquid ^{3}He, Physica B 284–288 (2000) 180–181.
[16] P.J. Nacher, G. Tastevin, B. Villard, N. Piegay, F. Marion, K. Sauer, NMR instabilities in spin-polarised liquids: ^{3}He, ^{3}He–^{4}He mixtures and ^{129}Xe, J. Low Temp. Phys. 121 (2000) 743–748.
[17] K.L. Sauer, F. Marion, P.J. Nacher, G. Tastevin, NMR instabilities and spectral clustering in laser-polarized liquid xenon, Phys. Rev. B 63 (2001), 184427, 1–4.
[18] J. Jeener, A. Vlassenbroek, P. Broekaert, Unified derivation of the dipolar field and relaxation terms in the Bloch–Redfield equations of liquid NMR, J. Chem. Phys. 103 (1995) 1309–1332.

[19] S. Lee, W. Richter, S. Vathyam, W.S. Warren, Quantum treatment of the effects of dipole–dipole interactions in liquid nuclear magnetic resonance, J. Chem. Phys. 105 (1996) 874–900.
[20] W.S. Warren, S. Ahn, The boundary between liquidlike and solidlike behavior in magnetic resonance, J. Chem. Phys. 108 (1998) 1313–1325.
[21] J. Jeener, Dynamical effects of the dipolar field inhomogeneities in high-resolution NMR: spectral clustering and instabilities, Phys. Rev. Lett. 82 (1999) 1772–1775.
[22] J.D. Walls, F.K.H. Phoa, Y.Y. Lin, Spin dynamics at very high spin polarization, Phys. Rev. B 70 (2004), 174410, 1–8.
[23] H.T. Edzes, The nuclear magnetization as the origin of transient changes in the magnetic field in pulsed NMR experiments, J. Magn. Reson. 86 (1990) 293–303.
[24] L. Dubois, P. Berthault, J.G. Huber, H. Desvaux, Mapping hydrophobic molecular regions using dissolved laser-polarized xenon NMR, C. R. Phys. 5 (2004) 305–313.
[25] H. Desvaux, T. Gautier, G. Le Goff, M. Pétro, P. Berthault, Direct evidence of a magnetization transfer between laser-polarized xenon and protons of a cage-molecule in water, Eur. Phys. J. D 12 (2000) 289–296.
[26] H.L. Clever, IUPAC Solubility Data Series, Pergamon Press, Oxford, 1979.
[27] H. Desvaux, R. Kümmerle, J. Kowalewski, C. Luchinat, I. Bertini, Direct measurement of dynamic frequency shift indued by cross-correlations in ^{15}N enriched proteins, ChemPhysChem 5 (2004) 959–965.
[28] W.H. Press, S.A. Teukolsky, W.T. Vetterling, B.P. Flannery, Numerical Recipes in C. The Art of Scientific Programming, Cambridge University Press, Cambridge, 1988.
[29] A. Abragam, Principles of Nuclear Magnetism, Clarendon Press, Oxford, 1961.
[30] P. Berthault, H. Desvaux, G. Le Goff, M. Pétro, A simple way to properly invert intense nuclear magnetization: application to laser-polarized xenon, Chem. Phys. Lett. 314 (1999) 52–56.
[31] J. Jeener, Equivalence between the "classical" and the "Warren" approaches for the effects of long range dipolar couplings in liquid nuclear magnetic resonance, J. Chem. Phys. 112 (2000) 5091–5094.
[32] M. Goldman, H. Desvaux, Cross-precession induced by the average dipolar field in high-resolution NMR, Chem. Phys. Lett. 256 (1996) 497–501.
[33] J.A. Osborn, Demagnetizing factors of the general ellipsoid, Phys. Rev. 67 (1945) 351–357.
[34] N. Segebarth, L. Aïtjeddig, E. Locci, K. Bartik, M. Luhmer, Novel method for the measurement of xenon gas solubility using ^{129}Xe NMR spectroscopy, J. Phys. Chem. A 110 (2006) 10770–10776.
[35] X.A. Mao, J.X. Guo, C.H. Ye, Nuclear magnetic resonance lineshape theory in the presence of radiation damping, Phys. Rev. B 49 (1994) 15702–15711.
[36] M.P. Augustine, Transient properties of radiation damping, Prog. NMR Spectrosc. 40 (2002) 111–150.
[37] S.J. Glaser, J.J. Quant, Homonuclear and heteronuclear Hartmann–Hahn transfer in isotropic liquids, in: W.S. Warren (Ed.), Adv. Magn. Opt. Reson, vol. 19, Academic Press Inc., San Diego, 1996, pp. 59–252.